Characteristics of Power and Cross Spectra of Wind Fluctuation along Meridian on Dome-like Structures

Yuan-Lung Lo[a], Jun Kanda[b]

[a] *The University of Tokyo, Kashiwa, Chiba, Japan, ohlalaloren@hotmail.com*
[b] *The University of Tokyo, Kashiwa, Chiba, Japan, kandaj@k.u-tokyo.ac.jp*

1 INTRODUCTION

Large-scale structures have been commonly constructed for various kinds of events in the past few decades. Among large-scale structures, dome-like roofs are most popularly designed. However, the curved geometry makes the estimation of wind pressure fluctuation a difficult task for wind resistant design. The curvature of dome roofs may strongly affect the flow pattern after the separation points or the occurrence of reattachment. Therefore the characteristics of pressure fluctuations on dome roofs from upstream to downstream demands further investigation for appropriate wind resistant design. Several researches have been conducted regarding this field. Toy et al (1983) showed that with the increased turbulent intensity, both separation and reattachment points move downstream. Ogawa et al (1991) investigated the characteristics of power and cross spectra and proposed location-dependent approximated models of power and cross spectra. Uematsu (1997 and 2008) researched the statistical nature of wind pressure coefficients and proposed an evaluation system for the cladding of spherical domes. Cheng and Fu (2010) investigated Reynolds number effect from 5.3×10^4 to 2.0×10^5 on hemispherical domes and calculated correlation length of pressure fluctuations for the locations of separation points.

This research intends to investigate the characteristics of power and cross spectra of wind pressure fluctuations by conducting a series of wind tunnel experiments. The variation of power spectra from upstream to downstream along the meridian of dome roofs and the coherence function of adjacent fluctuating pressures were investigated. The variations of phase functions due to locations were also investigated. For the appropriate wind resistant design of dome-like structures, it would be much beneficial to properly build up several flow patterns with respect to locations on dome roofs.

2 OUTLINES OF WIND TUNNEL EXPERIMENTS

The experiments were carried out in a turbulent boundary layer wind tunnel with a section of 15.6m (length) × 1.8m (width) × 1.8 (height). Urban turbulent flow was simulated by installing spires and roughness blocks along the development section. Figure 1 shows the mean wind velocity profile and turbulence intensity profile inside the wind tunnel, which are generally compatible with terrain IV in AIJ standards (power law index = 0.27). The velocity at boundary height (U_G) is about 9.85 m/sec. For the range of roof heights, turbulent intensity varies from 15.4% to 23.5%.

Figure 2 shows the geometric diagram of acrylic models and the arrangement of pressure taps. Every testing model is combined with a doom roof model and a cylinder model. Table 1 lists the nomenclature of testing models. The span of every dome roof is 300mm. The ratio of roof height to span (f/D) varies from 0.0 to 0.5 and the ratio of cylinder height to span (h/D) varies from 0.0 to 0.5. Except for the combination of f/D=0.0 and h/D=0.0, there are totally 35 testing models. Pressure taps are only installed along the

meridian of dome roof models. The Reynolds number defined by the span of the model, d, and wind velocity at the model height, U_H, is about 1.2×10^5.

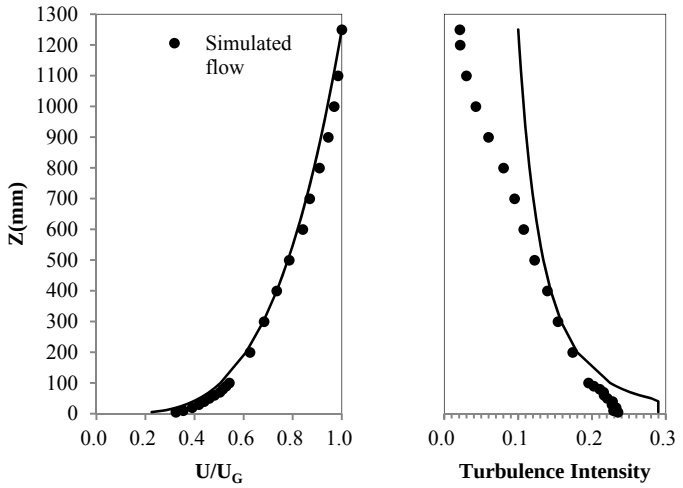

Figure 1 Profiles of simulated turbulent flow

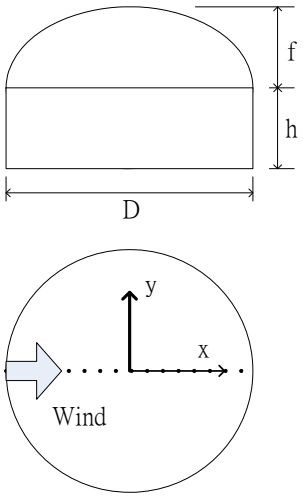

Figure 2 Geometric diagram of models

Table 1 Nomenclature of testing models

h/D \ f/D	0.0	0.1	0.2	0.3	0.4	0.5
0.0	---	B0	C0	D0	E0	F0
0.1	A1	B1	C1	D1	E1	F1
0.2	A2	B2	C2	D2	E2	F2
0.3	A3	B3	C3	D3	E3	F3
0.4	A4	B4	C4	D4	E4	F4
0.5	A5	B5	C5	D5	E5	F5

3 WIND PRESSURE COEFFICIENT DISTRIBUTIONS

3.1 *Mean and R.M.S. wind pressure coefficients*

Pressure coefficients are defined as Equation (1) where p_i and p_{ref} represent dynamic pressures and reference static pressures respectively. ρ is air density and U_H represents mean wind velocity at model height.

$$C_{p,i} = \frac{p_i - p_{ref}}{\frac{1}{2}\rho U_H^2} \tag{1}$$

Wind pressure measurements were conducted for 2 minutes in 1000 Hz. By assuming time scale 1/50, a 12 seconds in the wind tunnel is considered as a 10 minutes in field. The mean wind pressure coefficient of every tap along the meridian is the mean value of 10 segments of 12 seconds in the wind tunnel.

Figure 3 shows mean wind pressure coefficients along meridian of dome roofs. It is clearly observed that the distributions along the meridian become more distinct as the curvature of dome roof varies from f/D=0.1 to f/D=0.5. However, the case of f/D=0.0 (flat roof) is obviously different from curved roofs. Interestingly, f/D=0.1 with h/D larger than 0.3 not only shows the tendency of curved roofs but also that of flat roofs in the approaching edge. In every sub-figure, the increase of height makes a clear difference in general. From f/D=0.2 to f/D=0.5, the discontinuity occurrence in x/D=0.1~0.3 is observed, where may be considered as the occurrence of flow separation. As the curvature

increases, the separation becomes more distinct. Flow after the separation is coming to a consistence when f/D increases.

Figure 4 shows the distributions of R.M.S. wind pressure coefficients. As mean coefficient distributions, f/D=0.0 shows a quite different tendency from curved roofs and f/D=0.1 shows a similar tendency as flat roof in the approaching edge. The variation from f/D=0.2 to f/D=0.5 becomes more scattered; however, the increase of cylinder heights seems less dominant except for x/D=0.1~0.3.

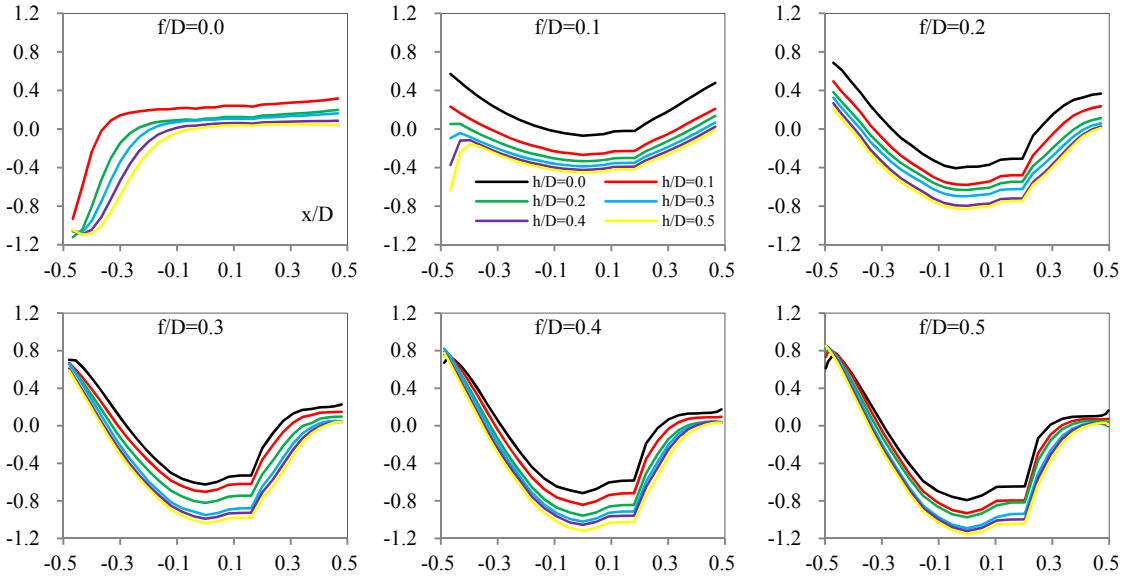

Figure 3 Mean wind pressure coefficient distributions along meridian

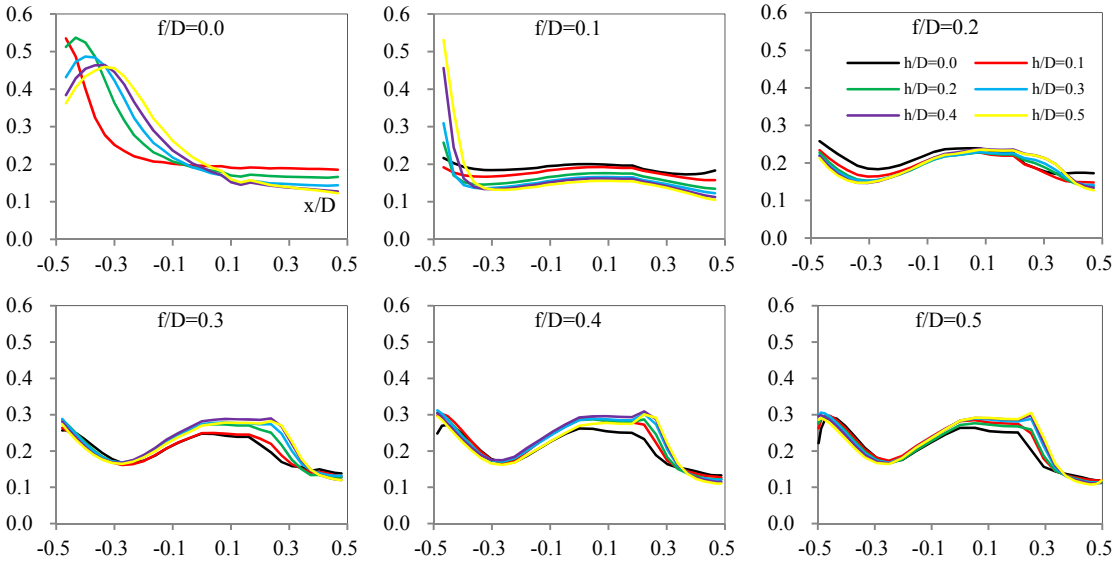

Figure 4 R.M.S. wind pressure coefficient distributions along meridian

3.2 *Cross correlation between two adjacent pressures along the meridian*

To further understand the changing characteristics of wind pressure fluctuations along the meridian from upstream to downstream, cross correlations between two adjacent pressures are calculated as Figure 5. For the overall roof of f/D=0.0 and the approaching edge of f/D=0.1, since the separation occurs at the edge of roof, the cross correlation signifi-

cantly varies from upstream to downstream. Besides, the increase of cylinder height affects clearly the extent of cross correlation.

For f/D=0.2~0.5, a sudden downshift can be observed at x/D=0.1~0.3, which is consistent with the distributions of mean wind pressure coefficients. Therefore, the separation may be considered occurred at x/D=0.1~0.3. However, it is still a difficult task to find the exact location of separation point is in this study. It is considered generally that as the curvature varies the separation point may move forward or backward.

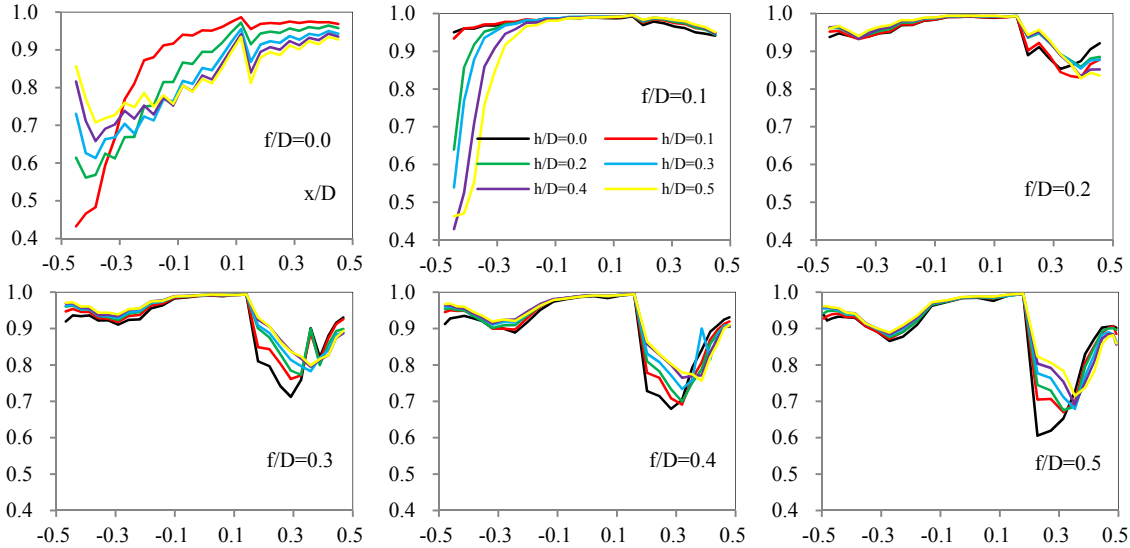

Figure 5 Cross correlation between two adjacent wind pressure fluctuations along the meridian

4 POWER AND CROSS SPECTRA OF WIND PRESSURE FLUCTUATIONS

4.1 *Power spectrum characteristics*

The approaching wind and the wake flow mutually dominate the fluctuation energy and show different patterns along the meridian from upstream to downstream. Power spectrum of wind pressures is then calculated to investigate the fluctuation energy distributed in the frequency domain. As Figure 6 shown, f/D=0.5 with h/D=0.2 shows roughly different patterns of power spectra.

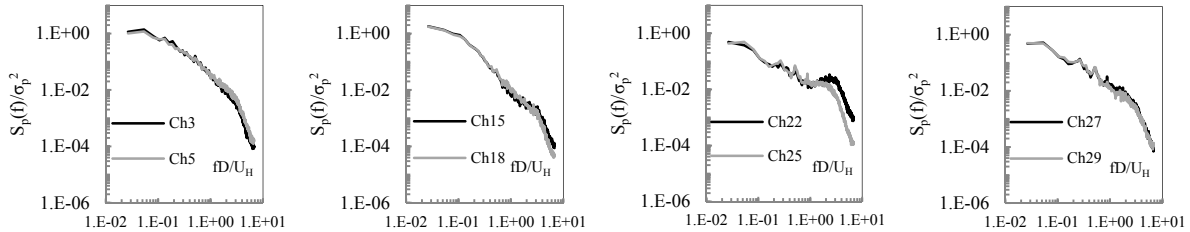

Figure 6 Normalized power spectra along the meridian in the case of f/D=0.5 with h/D=0.2

Normalized power spectra of channel No.3 and No.5 (in the upstream) are similar to the characteristics of approaching wind speed fluctuations. As the flow moves to the downstream, the apex at higher frequency range becomes more distinct. The apex vanishes later in the very rear downstream. The energy in the apex part may be affected by the approaching wind speed, the curvature of dome roofs, or the cylinder height. Several patterns of wind pressure fluctuations may be suggested depending on location.

To approximate the power spectrum characteristics of wind pressure fluctuations, the following equation is used for the lower frequency range for the first term and the higher frequency range for the second term. The location (a_1, a_2) and shape (c_1, c_2) parameters are approximated by solving nonlinear curve fitting in least square sense, which is provided in MATLAB built-in functions. The second term of equation (2) is modified from that proposed by Kumar and Stathopoulos (1997) to fit the apex part better.

$$\frac{S_p(f)}{\sigma_p^2} = a_1 e^{-c_1 f} + a_2 f e^{-c_2 f} \tag{2}$$

Figure 7 shows an example of approximation of a power spectrum (Channel No. 25, f/D=0.5 with h/D=0.2). The first term of approximation is considered affected by the approaching wind; meanwhile the second term may be used to simulate the effect of wake flows.

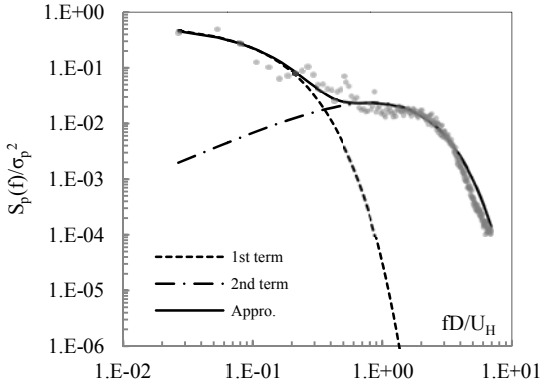

Figure 7 Approximation of channel No.25 in the case of f/D=0.5 with h/D=0.2
(a_1=0.6085, c_1=0.5377, a_2=0.0042, c_2=0.0654)

Figure 8 Parameters of power spectrum approximations along the meridian on f/D=0.2 dome roof

Figure 9 Parameters of power spectrum approximations along the meridian on f/D=0.5 dome roof

Figure 8 and 9 show the parameters, a_1, a_2, c_1, and c_2 of f/D=0.2 and 0.5 respectively. It is indicated that for the approximation of the first term, the differences caused by cylinder heights are more distinct than that of the second term. With the increase of f/D, the variations of a_2 and c_2 become less scattered except for the case of h/D=0.2.

4.2 *Cross spectrum characteristics*

Cross spectra of fluctuating wind pressures between channel No. i and No. j can be defined as equation (3) where $r_{i,j}(f)$ represents the root coherence and $\theta_{i,j}(f)$ represents the phase differences at No. i and j.

$$S_{p,i,j}(f)=\sqrt{S_{p,i}(f)S_{p,j}(f)}\cdot r_{i,j}(f)\cdot e^{i\theta_{i,j}(f)} \tag{3}$$

Figure 10 shows the distributions of root coherence and phase difference of two adjacent wind pressure fluctuations along the meridian on the case of f/D=0.5 with h/D=0.2. It is indicated that the distributions of root coherence and phase difference vary as the location of wind pressures moves from upstream to downstream.

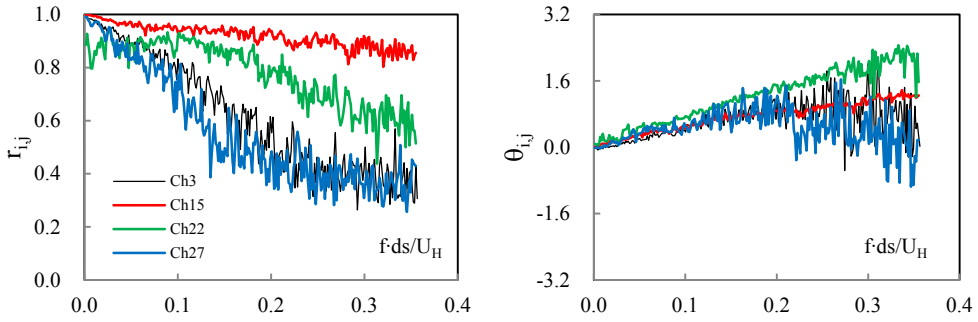

Figure 10 Root coherence and phase difference functions in the case of f/D=0.5 with h/D=0.2

In order to investigate the tendencies of root coherence and phase difference along the meridian, equation (4) and (5) are used for approximation. A detailed formula may be suggested in the future for the approximation in the very low normalized frequency range.

$$r_{i,j}(f)=e^{-k_1\left(\frac{f\cdot ds}{U_H}\right)} \tag{4}$$

$$\theta_{i,j}(f)=2\pi\cdot k_2\cdot\left(\frac{f\cdot ds}{U_H}\right) \tag{5}$$

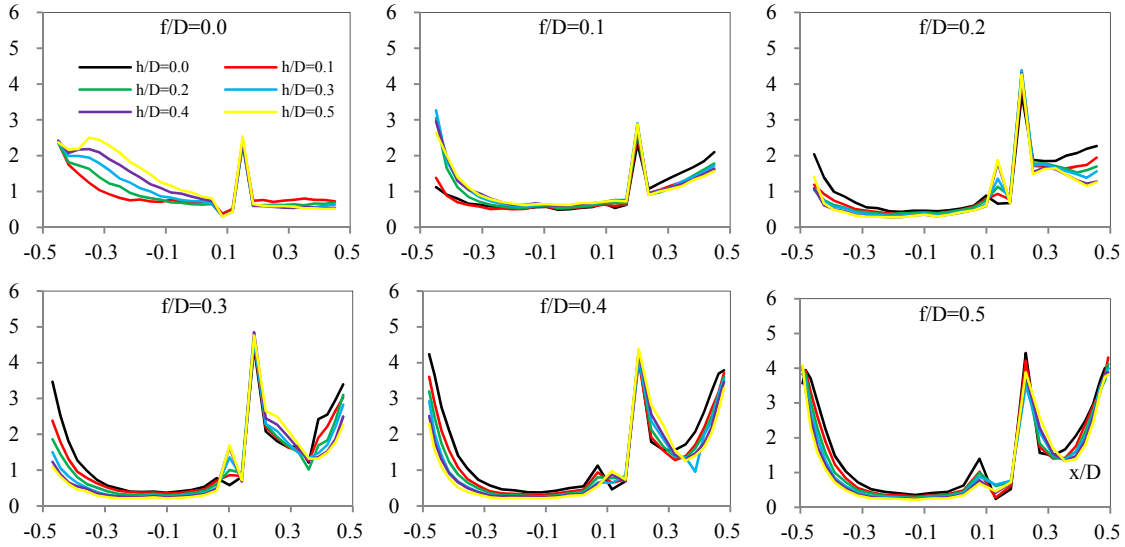

Figure 11 Root coherence functions between two adjacent wind pressure fluctuations along the meridian

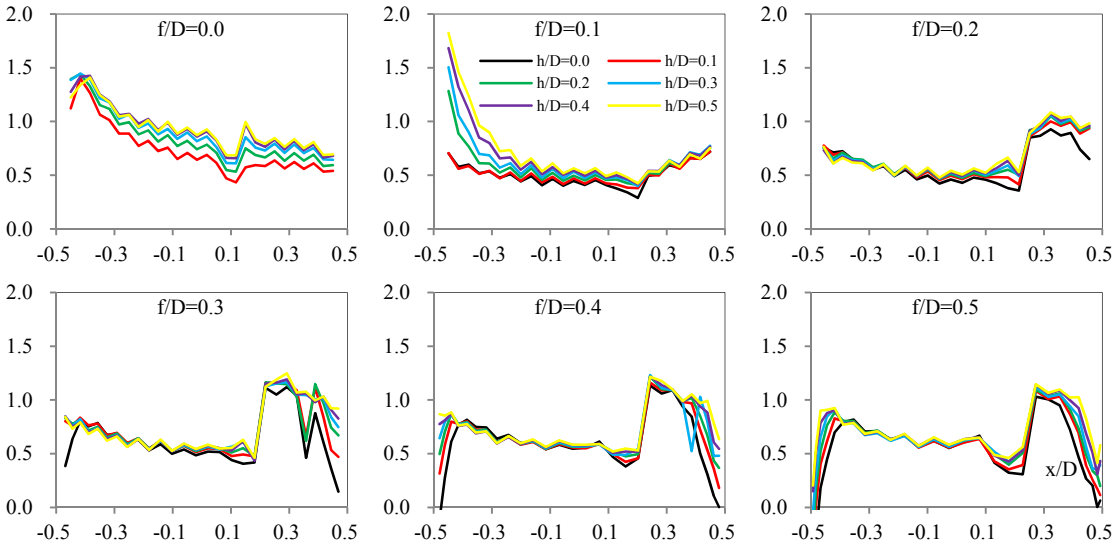

Figure 12 Phase difference functions between two adjacent wind pressure fluctuations along the meridian

Figure 11 and 12 shows the distributions of parameters of the approximation, k_1 and k_2, along the meridian. For the distributions of root coherence functions and phase differences, an apparent peak is observed at x/D=0.1~0.3, which indicates a dominant change of wind flow between two adjacent pressures. Compared to the observation of wind pressure coefficients, the changing of the wind flow is consistent. However, equation (4) and (5) may be criticized for the poor approximation in the very low normalized frequency range and may be meaningless if the scattering is significantly large in the higher normalized frequency range. Further, the linear approximation for phase difference functions may be insufficient in the higher normalized frequency range.

For simplicity, the characteristics of cross spectra on dome roofs have been modeled by co-coherence functions and only one universal approximation is proposed for any locations along the meridian (Uematsu, 1997). However, it is clearly observed from Figure 11 and 12, root coherence and phase difference functions may provide more detailed information and show the tendency better.

5 PRELIMINARY ZONING OF WIND PRESSURES ALONG THE MERIDIAN

A preliminary zoning of wind pressures may be suggested for further load resistant design based on the aforementioned investigation results. According to the tendencies shown in the wind pressure coefficients, power and cross spectra, several divisions may be roughly suggested.

From the mean wind pressure coefficients, the positive wind pressures are observed in curved dome roofs at x/D=-0.5~-0.3, where may be considered the effect of the approaching wind. For x/D=-0.3~0.5, although the negative mean wind pressure coefficients are observed, an extinct peak is generally distributed at x/D=0.1~0.3, where may be considered as the location of the separation occurrence. For x/D=0.3~0.5, the tendency becomes less significant. Distributions of R.M.S. wind pressure coefficients, cross correlations between two adjacent wind pressures, approximations of two terms of power spectra, and approximations of root coherence and phase difference functions may show similar divisions to help modeling the zoning of wind flow patterns.

The different tendencies shown in flat roofs or nearly flat roofs (f/D=0.1) may be considered as another system of wind flow pattern from those of curved roofs (f/D=0.2~0.5). Table 2 simply shows the case of f/D=0.1~0.5 with h/D=0.2. The divisions between dif-

ferent f/D may be difficult to clarify. However, the concept of zoning may still help modeling the wind flow patterns for wind load resistant design in the future.

Table 2 Preliminary zoning of the meridian on curved roofs with h/D=0.2

f/D	Region 1	Region 2	Region 3	Region 4
0.1	x/D = -0.500 ~ -0.432	-0.432 ~ 0.500	--	--
0.2	x/D = -0.500 ~ -0.375	-0.375 ~ 0.323	0.323 ~ 0.392	0.392 ~ 0.500
0.3	x/D = -0.500 ~ -0.342	-0.342 ~ 0.180	0.180 ~ 0.326	0.326 ~ 0.500
0.4	x/D = -0.500 ~ -0.338	-0.338 ~ 0.202	0.202 ~ 0.386	0.386 ~ 0.500
0.5	x/D = -0.500 ~ -0.335	-0.335 ~ 0.227	0.227 ~ 0.388	0.388 ~ 0.500

6 CONCLUSIONS

Experimental results indicated that the pattern of wind flow varies along the meridian from upstream to downstream. By investigating wind pressure coefficients, power and cross spectra of wind pressure fluctuations, the characteristics of wind flows on dome roofs were shown to be mathematically modeled. Approximations of power and cross spectra used in this paper provided a simple parametric study for the tendencies of wind pressure fluctuations. Though the rough fitting for root coherence and phase difference functions may be criticized, it helps to investigate the overall trends and clarify the pattern divisions of wind flows. Preliminary zoning along the meridian of curved roofs was attempted based on observed tendencies. For the practical wind load resistant design, modeling of wind flows in each division is expected and may be beneficial to modification of load standards.

7 ACKNOWLEDGEMENTS

Financial assistance for this research was provided in part by Kajima Foundation.

8 REFERENCES

Ogawa, T., Nakayama, M., Murayama, S., Sasaki, Y., 1991, Characteristics of wind pressure on basic structures with curved surfaces and their response in turbulent flow, Journal of Wind Engineering and Industrial Aerodynamics 38, 427-438.

Suresh Kumar, K., Stathopoulos, T., 1997, Computer simulation of fluctuating wind pressures on low building roofs, Journal of Wind Engineering and Industrial Aerodynamics 69-71, 485-495.

Toy, N., Moss, W.D., Savory, E., 1983, Wind tunnel studies on a dome in turbulent boundary layers, Journal of Wind Engineering and Industrial Aerodynamics 11, 201-212.

Uematsu, Y., Yamada, M., Inoue, A., Hongo, T., 1997, Wind loads and wind-induced dynamic behavior of a single-layer latticed dome, Journal of Wind Engineering and Industrial Aerodynamics 66, 227-248.

Uematsu, Y., Moteki, T., Hongo, T., 2008, Model of wind pressure field on circular flat roofs and its application to load estimation, Journal of Wind Engineering and Industrial Aerodynamics 96, 1003-1014.

Uematsu, Y., Tsuruishi, R., 2008, Wind load evaluation system for the design of roof cladding of spherical domes, Journal of Wind Engineering and Industrial Aerodynamics 96, 2054-2066.